# Nondynamic Kinetic Resolution of Configurationally Stable Biaryl Lactones by Reduction with Oxazaborolidine-Activated Borane: AM1 Studies and Experimental Verification†

Gerhard Bringmann,* Jürgen Hinrichs, Jürgen Kraus, Andreas Wuzik, and Tanja Schulz

*Institut für Organische Chemie, Universität Würzburg, Am Hubland, D-97074 Würzburg, Germany*

*Received November 4, 1999*

The complete mechanistic course of the atroposelective ring opening of a lactone-bridged biaryl, dinaphth[2,1-*c*:1′,2′-*e*]oxepin-3-(5*H*)-one (**3**), with a chiral oxazaborolidine−$BH_3$ complex was calculated using the semiempirical AM1 method. The first hydride transfer to the activated carbonyl function of the adduct complexes was elaborated to be the selectivity-determining step in the postulated five-step mechanism. The calculated enantioselectivity is in good accordance with the experimental results, so that related calculations were performed on the atroposelective ring opening of a sterically strongly hindered and therefore also configurationally stable six-membered biaryl lactone, 1,3-di-*tert*-butyl-6*H*-benzo[*b*]naphtho[1,2-*d*]pyran-6-one (**6f**). These calculations predicted a highly (*M*)-selective reduction of **6f** ($k_M/k_P = 358$ at −78 °C), which, after the smooth preparation of **6f** by intramolecular biaryl coupling in high yields, was fully confirmed experimentally ($k_M/k_P >$ 200 at −78 °C). Isolation of the intermediate hydroxy aldehyde (*M*)-**14** at the beginning of the reaction with the same enantiomeric excess as found for the corresponding alcohol (*M*)-**7f** conclusively showed the first hydride transfer step to determine the selectivity of this process. The good agreement of computationally predicted and experimentally confirmed values proves the suitability of the AM1 method for mechanistic studies on even such complex reactions and opens a most efficient overall synthesis of sterically highly hindered biaryls, in excellent chemical (for the ring closure) and optical (for the ring cleavage) yields and for any desired axial configuration.

## Introduction

Restricted rotation around a C−C bond is found in numerous natural products, e.g., in the nerve-growth-stimulating biphenyl mastigophorene A (**1**)[1] and the antispermatogenic binaphthyl (*M*)-gossypol (**2**),[2] giving rise to the existence of atropisomers with sometimes different pharmacological activities. Enantiomerically pure biaryl compounds are also of increasing value as axially chiral reagents and ligands in stereoselective synthesis.[3]

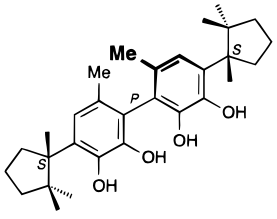


Mastigophorene A (**1**)

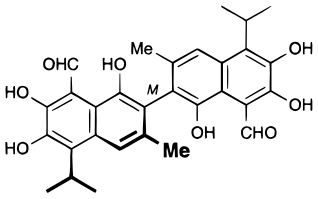


(*M*)-Gossypol (**2**)

For the construction of stereochemically homogeneous biaryl compounds, we have developed a potent methodology,[4] the atroposelective cleavage of configurationally labile biaryl lactone precursors using *O*-, *N*-, or *H*-nucleophiles.[5−7] This principle, which has meanwhile been applied to the synthesis of a broad series of bioactive biaryl natural products[4,8−10] and useful reagents,[11] has recently been extended to related but configurationally stable[12] seven-membered biaryl lactones such as **3**, resulting in a highly effective enantioselective formation, e.g., of (*M*)-**5** and unreacted (*P*)-**3**, with remarkably high relative rate constants ($k_{rel} = 50$).[13]A disadvantage of the method is that this is just a "normal", i.e., *non*dynamic kinetic resolution, because—different from the configurationally unstable six-membered lactones **6**—the atropisomerization barrier of **3** is so high that there is no continuous supply of the more rapidly reacting enanti-

* Corresponding author. E-mail: bringman@chemie.uni-wuerzburg.de.

† Part 86 of the series "Novel Concepts in Directed Biaryl Synthesis". For part 85, see ref 10.

(1) (a) Fukuyama, Y.; Asakawa, Y. *J. Chem. Soc., Perkin Trans. 1* **1991**, 2737. (b) Bringmann, G.; Pabst, T.; Busemann, S.; Peters, K.; Peters, E.-M. *Tetrahedron* **1998**, *54*, 1425. (c) Bringmann, G.; Pabst, T.; Rycroft, D. S.; Connolly, J. D. *Tetrahedron Lett.* **1999**, *40*, 483. (d) Degnan, A. P.; Meyers, A. I. *J. Am. Chem. Soc.* **1999**, *121*, 2762.

(2) Cass, Q. B.; Tiritan, E.; Matlin, S. A.; Freire, E. C. *Phytochemistry* **1991**, *30*, 2655 and references therein.

(3) (a) Rosini, C.; Franzini, L.; Raffaelli, A.; Salvadori, P. *Synthesis* **1992**, 503. (b) Pu, L. *Chem. Rev.* **1998**, *98*, 2405.

(4) Bringmann, G.; Breuning, M.; Tasler, S. *Synthesis* **1999**, 525.

(5) (a) Bringmann, G.; Breuning, M.; Walter, R.; Wuzik, A.; Peters, K.; Peters, E.-M. *Eur. J. Org. Chem.* **1999**, 3047. (b) Seebach, D.; Jaeschke, G.; Gottwald, K.; Matsuda, K.; Formisano, R.; Chaplin, D. A.; Breuning, M.; Bringmann, G. *Tetrahedron* **1997**, *53*, 7539. (c) Bringmann, G.; Breuning, M.; Tasler, S.; Endress, H.; Ewers, C. L. J.; Göbel, L.; Peters, K.; Peters, E.-M. *Chem. Eur. J.* **1999**, *5*, 3029.

(6) Bringmann, G.; Hartung, T. *Tetrahedron* **1993**, *49*, 7891.

(7) Bringmann, G.; Breuning, M. *Tetrahedron: Asymmetry* **1999**, *10*, 385.

(8) (a) Bringmann, G.; Holenz, J.; Weirich, R.; Rübenacker, M.; Funke, C.; Boyd, M. R.; Gulakowski, R. J.; François, G. *Tetrahedron* **1998**, *54*, 497. (b) Bringmann, G.; Saeb, W.; Rübenacker, M. *Tetrahedron* **1999**, *55*, 423.

(9) Bringmann, G.; Ochse, M. *Synlett* **1998**, 1294.

(10) Bringmann, G.; Ochse, M.; Götz, R. *J. Org. Chem.*, in press.

(11) (a) Bringmann, G.; Breuning, M. *Tetrahedron: Asymmetry* **1998**, *9*, 667. (b) Bringmann, G.; Wuzik, A.; Breuning, M.; Henschel, P.; Peters, K.; Peters, E.-M. *Tetrahedron: Asymmetry* **1999**, *10*, 3025.

(12) Bringmann, G.; Hartung, T.; Kröcher, O.; Gulden, K.-P.; Lange, J.; Burzlaff, H. *Tetrahedron* **1994**, *50*, 2831.

(13) Bringmann, G.; Hinrichs, J. *Tetrahedron: Asymmetry* **1997**, *8*, 4121.

10.1021/jo991729x CCC: $19.00 
Published on Web 03/23/2000

**Scheme 1**

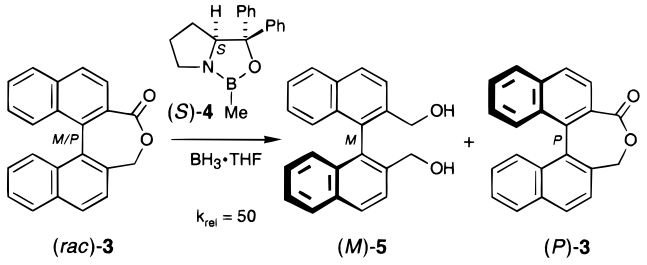


omer [here (*M*)-**3**] from the less reactive one [here (*P*)-**3**] at room temperature. On the other hand, the nondynamic kinetic resolution permits, in principle, an enrichment of the nonreactive enantiomer of the lactone [(*P*)-**3** for (*S*)-**4** or (*M*)-**3** for (*R*)-**4** as the reagent] up to optical *purity*.[13] Moreover, even if only one stereoisomeric product, e.g., only (*M*)-**5**, is needed, the less reactive atropisomer of **3** [here (*P*)-**3**] is not lost but can be recycled by thermal racemization and renewed enantioselective reduction.

In this paper, we report on the semiempirical AM1 calculation of the mechanistic course of the kinetic resolution of **3** and on the extension of the principle, both computationally and experimentally, to the even more efficient atropo-enantioselective cleavage of a configurationally stable six-membered biaryl lactone, as a most effective pathway to highly hindered biaryls of any desired configuration and optical purity.

## Results and Discussion

In recent papers we have presented quantum chemical studies on structures and dynamics of six-membered lactones such as **6**,[14,15] including the complete mechanistic course of the atropisomer-selective ring cleavage reaction of the configurationally unstable 1,3-dimethyl-6*H*-benzo[*b*]naphtho[1,2-*d*]pyran-6-one (**6c**) with a chiral oxazaborolidine−$BH_3$ complex[16] and with a chiral metalated *N*-nucleophile,[17] using the semiempirical AM1 and PM3 methods, respectively. As in our previous computational studies on configurationally unstable six-membered lactones,[16] we have subdivided the mechanistic course of the atroposelective ring cleavage of the configurationally stable seven-membered lactone **3** into five fundamental steps [Scheme 3, exemplarily for (*M*)-**3**], starting with the formation of the adduct **8** of **3** and the oxazaborolidine borane complex (*S*)-**4**·$BH_3$[18] (step **I**), which is followed by the first intramolecular nucleophilic attack (step **II**) of the activated hydride species to give lactolates of type **9** [here (*S*,*M*)-**9**]. In the following step **III**, the four-membered diboraheterocycle in **9** rearranges to give **10**, both oxygen atoms of the former lactone function now being part of a six-membered heterocycle. After the ring cleavage to form hydroxy aldehyde adducts **11** (step **IV**), the completing step **V**, the (presumably likewise intramolecular) second nucleophilic hydride transfer at the reinstalled carbonyl function of **11**, finally provides the diolates **12**, from which the ultimately isolated free diols **5** are set free by hydrolytic workup.

**Scheme 2**

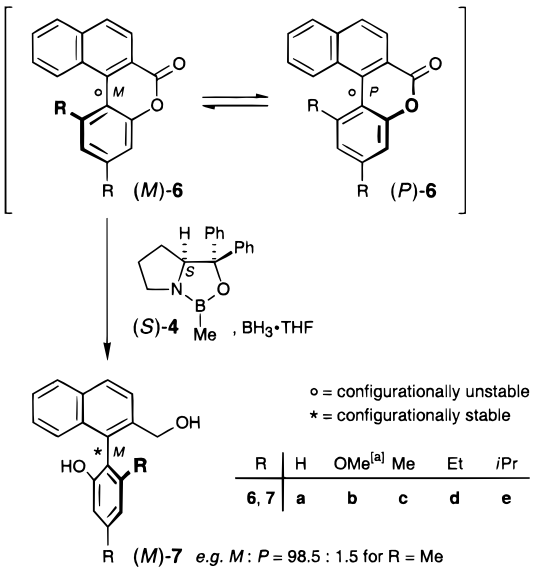


[a]Note that for formal reasons of the CIP denotation, stereochemically analogous biaryls of this series with R = OMe will have opposite descriptors compared to those with R = H or alkyl

**Scheme 3**

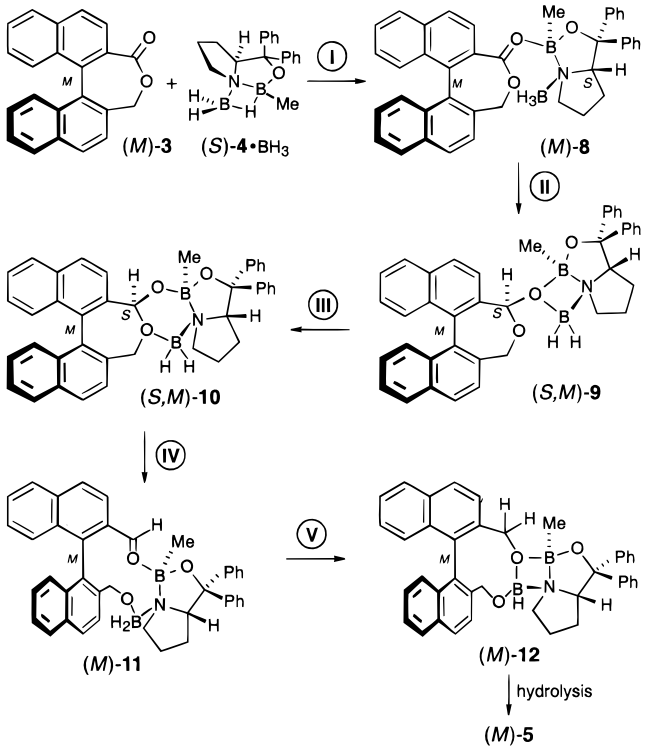


**First Fundamental Step: Formation of the Adduct Complexes 8.** The investigation of the first elemental step made it necessary to calculate reaction coordinates for the Lewis acid−Lewis base interactions between **3** and oxazaborolidine borane complex (*S*)-**4**·$BH_3$ (see Scheme 3), which during their approximation show an early energetic minimum **13** at a distance of approximately 7 Å between the carbonyl oxygen of **3** and the endocyclic boron atom of (*S*)-**4**·$BH_3$ [for each of the two atropisomers, (*M*)-**13** and (*P*)-**13**, two minimum structures were found, see Scheme 4 and Table 1; for the

(14) Bringmann, G.; Busse, H.; Dauer, U.; Güssregen, S.; Stahl, M. *Tetrahedron* **1995**, *51*, 3149.
(15) Bringmann, G.; Dauer, U.; Kraus, J. *Tetrahedron* **1998**, *54*, 12265.
(16) Bringmann, G.; Vitt, D. *J. Org. Chem.* **1995**, *60*, 7674.
(17) Bringmann, G.; Güssregen, S.; Vitt, D.; Stowasser, R. *J. Mol. Model.* **1998**, *4*, 165.
(18) Corey, E. J.; Azimioara, M.; Sarshar, S. *Tetrahedron Lett.* **1992**, *33*, 3429.

**Scheme 4**

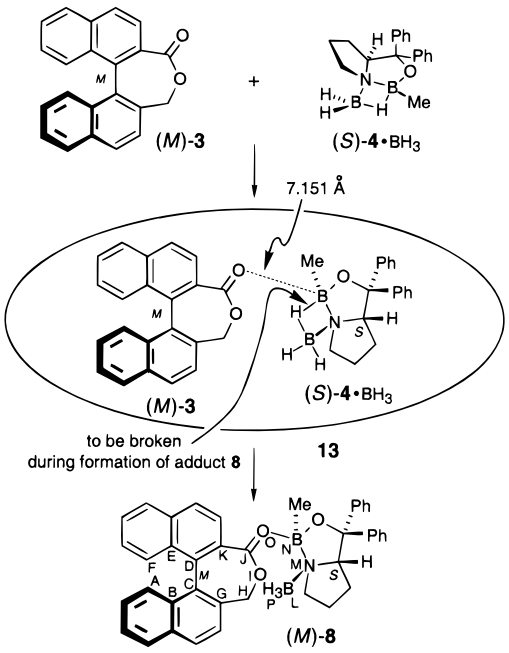


A, B, C, ...: atom denotation used throughout the text for **8** and related compounds

**Table 1. Heats of Formation ($\Delta H_f$, kcal/mol), Relative Heats of Formation ($\Delta\Delta H_f$, kcal/mol), and Selected Bond Lengths (Å) of the Energetically Lowest Conformations of Mechanistic Intermediates 13**

| | $\Delta H_f$ | $\Delta\Delta H_f$ | $C_J-O_I$[a] | $B_L-O_I$ | $B_L-O_O$ | $B_N-O_O$ |
|---|---|---|---|---|---|---|
| (*M*)-**13** | −5.4 | 0.0 | 1.375 | 8.072 | 7.458 | 7.151 |
| (*M*)-**13** | −5.3 | 0.1 | 1.375 | 8.145 | 7.188 | 7.055 |
| (*P*)-**13** | −5.4 | ≡ 0 | 1.375 | 7.943 | 7.166 | 6.939 |
| (*P*)-**13** | −5.2 | 0.2 | 1.375 | 8.668 | 7.772 | 8.348 |

[a] For the atom denotation, see Scheme 4. For selected dihedral angles, see Supporting Information.

structures of **13**, see Supporting Information]. A further reduction of the $B_N$-$O_O$ distance (for the atom denotation used throughout this paper, see Scheme 4) of these weakly bonded Coulomb pairs **13** down to ca. 1.8 Å leads to a cleavage of the hydride-bridged structure of (*S*)-**4**·$BH_3$ (as marked in Scheme 4) and the formation of the adduct complexes **8**.

For each of the two atropisomers, (*M*)-**8** and (*P*)-**8**, three minimum structures were found (Table 2). All of their energies are distinctly (by 11−13 kcal/mol, see Tables 1 and 2) higher than those of **13**, as a result of larger steric crowding in **8** (compare Scheme 4) and the low stability of the new $B_N$-$O_O$ interaction compared to that of the previous hydride-bridged structure in **13**. The influence of the chirality of the oxazaborolidine (*S*)-**4** on the stability of the respective atropisomer, which does not yet become manifest in the calculated heats of formation ($\Delta H_f$) of the diastereomeric Coulomb pairs (*M*)- and (*P*)-**13** ($\Delta\Delta H_f$ < 0.1 kcal/mol, see Table 1), can clearly be seen for the adducts (*M*)- and (*P*)-**8**; the difference between the energetically lowest conformers of the adducts (*M*)-**8** and (*P*)-**8** (presented in Figure 1) amounts to the notable value of 2.1 kcal/mol (7.5 − 5.4 kcal/mol, Table 2).

The complexation of the biaryl lactone **3** to the oxazaborolidine borane complex (*S*)-**4**·$BH_3$ leads to an

**Table 2. Heats of Formation ($\Delta H_f$, kcal/mol), Relative Heats of Formation ($\Delta\Delta H_f$, kcal/mol), and Selected Bond Lengths (Å) of the Mechanistic Intermediates 8−12**

| | $\Delta H_f$ | $\Delta\Delta H_f$ | $C_J-O_I$[a] | $B_L-O_I$ | $B_L-O_O$ | $B_N-O_O$ |
|---|---|---|---|---|---|---|
| (*M*)-**8** | 7.8 | 0.3 | 1.357 | 3.147 | 2.919 | 1.832 |
| (*M*)-**8** | 8.0 | 0.5 | 1.374 | 4.610 | 2.988 | 1.924 |
| (*M*)-**8** | 7.5 | ≡ 0 | 1.358 | 3.377 | 2.896 | 1.842 |
| (*P*)-**8** | 5.4 | ≡ 0 | 1.357 | 3.140 | 2.893 | 1.826 |
| (*P*)-**8** | 9.8 | 4.4 | 1.375 | 4.572 | 3.027 | 1.930 |
| (*P*)-**8** | 9.3 | 3.9 | 1.357 | 3.252 | 2.983 | 1.844 |
| (*S*,*M*)-**9** | −32.3 | ≡ 0 | 1.441 | 3.726 | 1.606 | 1.663 |
| (*R*,*M*)-**9** | −31.3 | 1.0 | 1.422 | 2.604 | 1.629 | 1.661 |
| (*S*,*P*)-**9** | −31.5 | ≡ 0 | 1.421 | 3.036 | 1.670 | 1.624 |
| (*R*,*P*)-**9** | −28.9 | 2.6 | 1.411 | 3.713 | 1.614 | 1.680 |
| (*S*,*M*)-**10** | −16.9 | 4.5 | 1.476 | 1.762 | 2.630 | 1.509 |
| (*R*,*M*)-**10** | −21.4 | ≡ 0 | 1.489 | 1.725 | 2.860 | 1.503 |
| (*S*,*P*)-**10** | −21.3 | ≡ 0 | 1.483 | 1.764 | 2.569 | 1.515 |
| (*R*,*P*)-**10** | −10.4 | 10.9 | 1.456 | 1.787 | 2.652 | 1.502 |
| (*M*)-**11** | −18.6 | ≡ 0 | 2.267 | 1.474 | 2.954 | 1.742 |
| (*M*)-**11** | −10.4 | 8.2 | 2.335 | 1.512 | 2.776 | 1.766 |
| (*P*)-**11** | −18.4 | ≡ 0 | 2.834 | 1.499 | 2.945 | 1.782 |
| (*P*)-**11** | −13.4 | 5.0 | 2.267 | 1.450 | 3.060 | 1.679 |
| (*M*)-**12** | −62.2 | ≡ 0 | 2.804 | 1.422 | 1.630 | 1.627 |
| (*M*)-**12** | −54.8 | 7.4 | 3.016 | 1.420 | 1.625 | 1.612 |
| (*P*)-**12** | −61.3 | ≡ 0 | 2.782 | 1.427 | 1.634 | 1.633 |
| (*P*)-**12** | −55.2 | 6.1 | 3.331 | 1.407 | 1.588 | 1.642 |

[a] For the atom denotation, see Scheme 4. For selected dihedral angles, see Supporting Information.

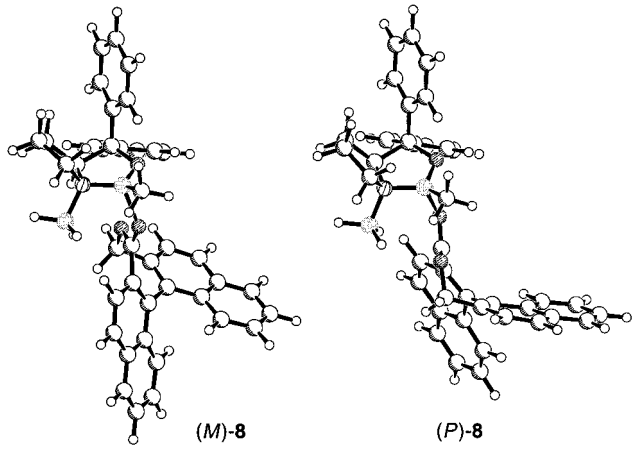


**Figure 1.** The two energetically lowest (out of six) minimum structures of the adduct **8**.

effective activation of both reaction partners[19] in the adduct **8**. As a result of the formal positive charge on the carbonyl oxygen in **8**, the electron density of the carbonyl carbon atom is reduced, favoring a nucleophilic attack by a hydride of the coordinated borane, whose negative partial charge is increased significantly compared to that of uncoordinated, free $BH_3$. This facilitates the reduction of the lactone **3** by an effective *synergetic cooperation*[20] between the catalyst (*S*)-**4**, the reduction equivalent $BH_3$, and the substrate lactone **3**.

At each stage of the reaction pathway, an uncontrolled atropisomerization might lead to an equilibration of the two respective atropisomers and thus to the loss of stereochemical information at the biaryl axis, the "stereochemical leakage",[4,16] and that should be strictly avoided. Calculated helimerization energy surfaces,[14] with activa-

(19) Corey, E. J.; Helal, C. J. *Angew. Chem., Int. Ed. Engl.* **1998**, *37*, 1986.
(20) Nevalainen, V. *Tetrahedron: Asymmetry* **1991**, *2*, 63.

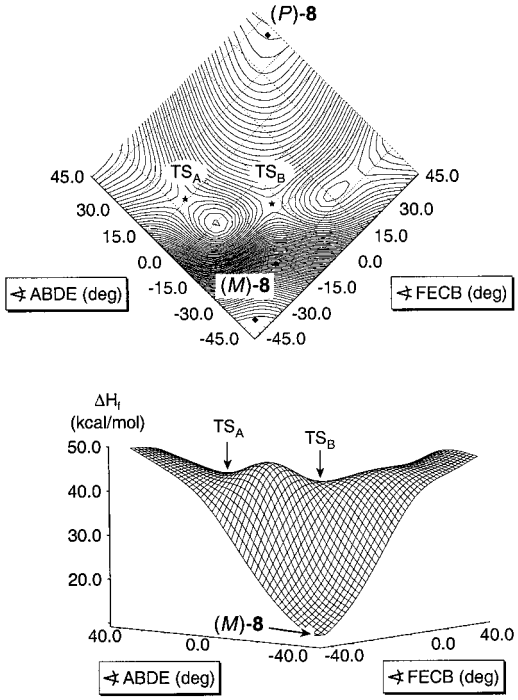


**Figure 2.** 2D plot and 3D energy surface visualization of the helimerization [(*M*)-**8** ⇌ (*P*)-**8**] in dependence of two dihedral angles (for the atom denotation, see Scheme 4).

tion barriers for the two diastereomeric transition structures TS [(*M*)-**8** ⇌ (*P*)-**8**]$_A$ and TS [(*M*)-**8** ⇌ (*P*)-**8**]$_B$ (see Figure 2) of 39.0 and 39.7 kcal/mol, reveal the adducts **8** to be configurationally stable at the axis. Atropisomeric interconversion is therefore in no way in competition with the following, distinctly more rapid (and irreversible) first reduction step (see below).

**Second Fundamental Step: First Intramolecular Nucleophilic Attack.** In the next fundamental step, the carbonyl function of the adducts **8** is subject to an intramolecular nucleophilic attack (step **II**, see Scheme 3). The new benzylic stereocenter of **9**, the previous carbonyl C-atom, is only of temporary interest to the total reaction, because it will be destroyed during the ring cleavage reaction that follows the isomerization from **9** to **10**.

The hydride transfer to the carbonyl function should, in analogy to earlier theoretical work by our group,[16] occur from an axial rather than from an equatorial direction, which in this case would mean a preferred attack on (*M*)-**3** from the *Si* face or on (*P*)-**3** from the *Re* face (compare Scheme 5, formulated for $H^-$ as an idealized hydride transfer reagent).

The calculated results (see Table 3) reveal a preferred *Si* attack on (*M*)-**3** with the energetically lowest activation barrier of 4.2 kcal/mol and thus prove the assumption of an axial attack. Interestingly, the energetically preferred analogous attack on the (*P*)-helimer of **3** (activation barrier 7.0 kcal/mol) also proceeds from the *Si* face, hence now in an equatorial manner [see Table 3, for the corresponding transition structures of (*M*,*Si*)-[**8** → **9**] and (*P*,*Si*)-[**8** → **9**] see Figure 3]. Both energetically favored transition structures adopt a chair conformation, as already evident from semiempirical calculations on related systems by Liotta[21] and from ab initio investigations by Quallich,[22] whereas Corey[23] and Evans[24] proposed a boatlike conformation for the transition state.

**Scheme 5**

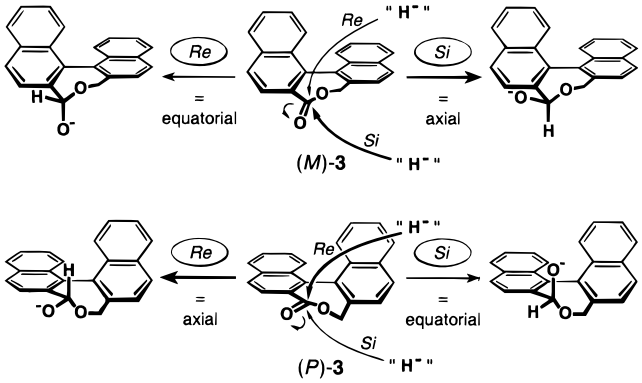


**Table 3. First Intramolecular Nucleophilic Attack: Heats of Formation ($\Delta H_f$, kcal/mol), Zero Point Energies (ZPE, kcal/mol), Imaginary Frequencies ($\nu_i$, $i \cdot cm^{-1}$), Activation Barriers ($\Delta H^{\ddagger}$), and Selected Bond Lengths (Å) of Transition Structures [8 → 9]**

| | [**8** → **9**] | | | | |
|---|---|---|---|---|---|
| | (*M*,*Si*) | (*M*,*Re*) | (*P*,*Si*) | (*P*,*Re*)$_A$[b] | (*P*,*Re*)$_B$[b] |
| direction of $H^-$-attack | axial | equatorial | equatorial | axial | axial |
| $\Delta H_f$ | 11.7 | 13.8 | 12.3 | 13.7 | 13.2 |
| $\Delta H^{\ddagger}$ | 4.2 | 6.3 | 7.0 | 8.3 | 7.8 |
| $\Delta\Delta H^{\ddagger}$ | ≡ 0 | 2.1 | 2.8 | 4.1 | 3.6 |
| ZPE | 438.7 | 438.6 | 438.6 | 438.8 | −381.4 |
| $\nu_i$ | −437.0 | −489.8 | −506.8 | −410.4 | −381.4 |
| $B_N-O_O$[a] | 1.711 | 1.650 | 1.655 | 1.746 | 1.717 |
| $B_L-H_P$ | 1.255 | 1.278 | 1.279 | 1.252 | 1.251 |
| $C_J-H_P$ | 1.695 | 1.558 | 1.573 | 1.674 | 1.699 |

[a] For the atom denotation, see Scheme 4. [b] The (*P*,*Re*)-attack was found to pass two transition structures [**8** → **9**], denoted by A and B.

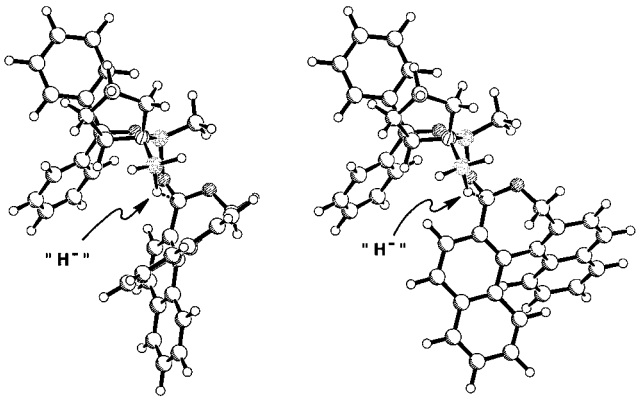


**Figure 3.** The two energetically favored transition structures [**8** → **9**] of the first nucleophilic attack on the carbonyl function of lactone **3**.

The first hydride transfer is fast and strongly exothermic [$\Delta H_f$ (**9**) − $\Delta H_f$ (**8**) ≈ 40 kcal/mol, see overall energy diagram in Scheme 7, vide infra] and thus irreversible.

(21) Jones, D. K.; Liotta, D. C.; Shinkai, I.; Mathre, D. J. *J. Org. Chem.* **1993**, *58*, 799.
(22) Quallich, G. J.; Blake, J. F.; Woodall, T. M. *J. Am. Chem. Soc.* **1994**, *116*, 8516.
(23) Corey, E. J.; Bakshi, R. K.; Shibata, S. *J. Am. Chem. Soc.* **1987**, *109*, 5551.
(24) Evans, D. A. *Science* **1988**, *240*, 420.

**Scheme 6**

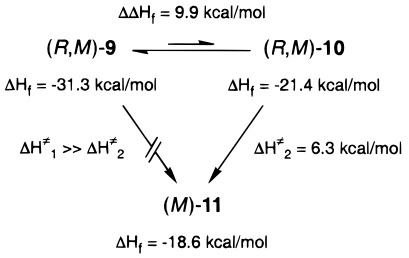


The stereoselectivity observed in this first, irreversible reduction step is in principle a combination of three formal selectivities of which two each determine the third one: an axial vs equatorial control, a diastereo face differentiation ("*Re*/*Si* control"), and an atropisomer differentiation (*M*/*P* selectivity). Of the four possible reaction pathways, *P*, *Si* (equatorial), *P*, *Re* (axial), *M*, *Re* (equatorial), and *M*, *Si* (axial), the latter mode is energetically preferred here over the lowest transition structure for an attack to the (*P*)-atropisomer, (*P*,*Si*)-[**8** → **9**]. This leads to a relative energetic difference $\Delta\Delta H^{\ddagger}$ in the activation barriers of 2.8 kcal/mol in favor of the reduction of lactone (*M*)-**3**, already during this first reductive step (see Table 3); even the equatorial attack to *M*, via (*M*,*Re*)-[**8** → **9**], is slightly favored over the *P*-attack. To check whether this irreversible step determines the selectivity of the overall process, the helimerization barriers of all mechanistically "later" reaction intermediates had to be calculated, thus excluding the possibility of an a posteriori loss of an initially attained selectivity by a stereochemical leakage,[16] caused by an imaginable configurational instability of the stereogenic biaryl axis. Lactol **9** was found to be configurationally stable at room temperature, with the calculated activation barriers for the helimerization of (*M*)-**9** to (*P*)-**9** and reverse both being >36 kcal/mol.

**Third Fundamental Step: Rearrangement of the Diboraheterocycle.** The second hydride transfer (step **V**) requires the reconstruction of the carbonyl function to give the hydroxy aldehyde adduct **11** (Scheme 3). From the lactol **9**,[25] there are two possible pathways to **11** (Scheme 6). The energy barrier for the "direct" ring cleavage of **9** to give **11** is much too high to be overcome; energetically far more favorably, the four-membered diboraheterocycle in **9** first isomerizes in an endothermic reaction to give a six-membered heterocycle in **10** (step **III**, Scheme 3), which is then ring-opened to form the hydroxy aldehyde **11** (step **IV**, Scheme 3).This isomerization from **9** to **10** is based on a simple change in the coordination sphere of the remaining $BH_2$ fragment, in the way that it migrates from the *exo*-oxygen in **9** to the *endo*-oxygen in **10**. The involvement of the ring oxygen leads to an electronic saturation of the $BH_2$ group. The heat of formation for the energetically most favored lactol (*R*,*M*)-**10** is −21.4 kcal/mol (see Table 2). It is thus by 10.9 kcal/mol less stable than the energetically lowest four-membered diboraheterocycle (*S*,*M*)-**9** ($\Delta H_f = -32.3$ kcal/mol, data shown in Table 2). This high energetic difference between the lactols **9** and **10** is based on the sterically inflexible *cis*-arrangement of the $BH_2$-group boron atom and the former carbonyl oxygen in the six-membered diboraheterocycle of lactol **10** (see Figure 4).

(25) Bringmann, G.; Hartung, T. *Angew. Chem., Int. Ed. Engl.* **1992**, *31*, 761.

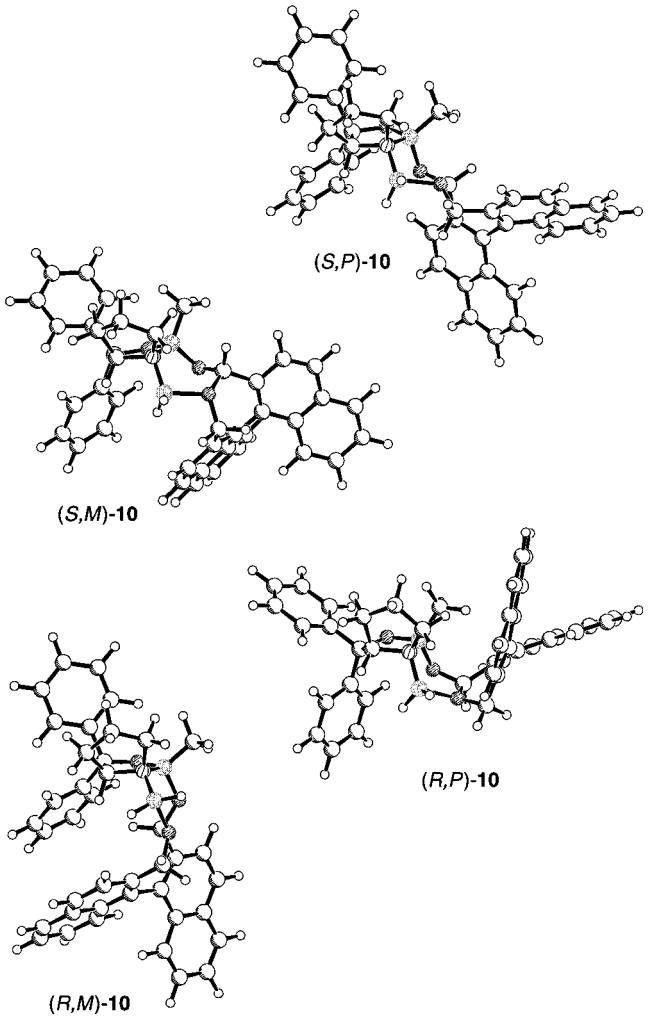


**Figure 4.** 3D minimum structures of the four possible diastereomeric lactols **10**, containing a six-membered diboraheterocycle.

The generated benzylic stereocenter in **9** (and **10**) will be destroyed during the following step **IV** of the ring opening reaction. As evident from the calculations, the lactols **10** are also configurationally stable at room temperature, with an activation barrier for the atropisomerization of >36 kcal/mol.

**Fourth Fundamental Step: Ring Opening Reaction.** In step **IV**, the slightly endothermic opening of the lactol ring of **10** leads to the hydroxy aldehyde **11**, with an 11-membered heterocycle containing the reconstructed (still boron-activated) carbonyl function, on which then the second hydride transfer (step **V**) can occur (Scheme 3). The coordinative bond between the *endo*cyclic oxygen and the *exo*cyclic boron in **10** is transformed into a covalent bond, thus permitting a direct compensation of the originating negative charge on the benzylic oxygen. This is the reason for the low activation barriers for this fundamental step, typically only 6.3 kcal/mol for (*M*)-[**10** → **11**]$_B$ (for both configurations at the biaryl axis, two transition structures were found and denoted by the indices A and B, see Table 4). All four transition structures [**10** → **11**] of this step **IV** pass through a twist-boat conformation (compare Figure 5).

Different conformers of **11**, although with the same configuration at the stereogenic axis, show extreme energetic differences in their heats of formation (up to

**Table 4. Heats of Formation ($\Delta H_f$, kcal/mol), Relative Heats of Formation ($\Delta\Delta H_f$, kcal/mol), Zero Point Energies (ZPE, kcal/mol), Imaginary Frequencies ($\nu_i$, $i$·cm$^{-1}$), Activation Barriers ($\Delta H^{\ddagger}$), Selected Bond Lengths (Å), and Dihedral Angles (deg) of Transition Structures [10 → 11]**

| | [10 → 11] | | | |
|---|---|---|---|---|
| | $(M)_A$ | $(M)_B$ | $(P)_A$ | $(P)_B$ |
| $\Delta H_f$ | −8.1 | −15.1 | −14.1 | 2.6 |
| $\Delta\Delta H_f$ | 7.0 | ≡ 0 | 0.8 | 17.7 |
| $\Delta H^{\ddagger}$ | 13.4 | 6.3 | 7.2 | 24.0 |
| ZPE | 440.1 | 439.5 | 439.8 | 439.6 |
| $\nu_i$ | −296.7 | −336.5 | −327.9 | −291.4 |
| $C_J-O_O$[a] | 1.294 | 1.301 | 1.300 | 1.276 |
| $B_L-O_I$ | 1.570 | 1.559 | 1.568 | 1.527 |
| $B_L-N_M$ | 1.595 | 1.595 | 1.598 | 1.624 |
| ∠ $O_I-B_L-N_M-B_N$ | 55.6 | −42.1 | 41.7 | 42.3 |
| ∠ $C_J-O_O-B_N-N_M$ | −72.1 | 48.8 | −88.4 | −75.6 |
| ∠ $B_L-O_I-C_J-O_O$ | −18.7 | 49.8 | 15.5 | −3.4 |
| ∠ $B_L-N_M-B_N-O_O$ | −8.1 | 25.0 | 18.8 | 2.4 |

[a] For the atom denotation, see Scheme 4.

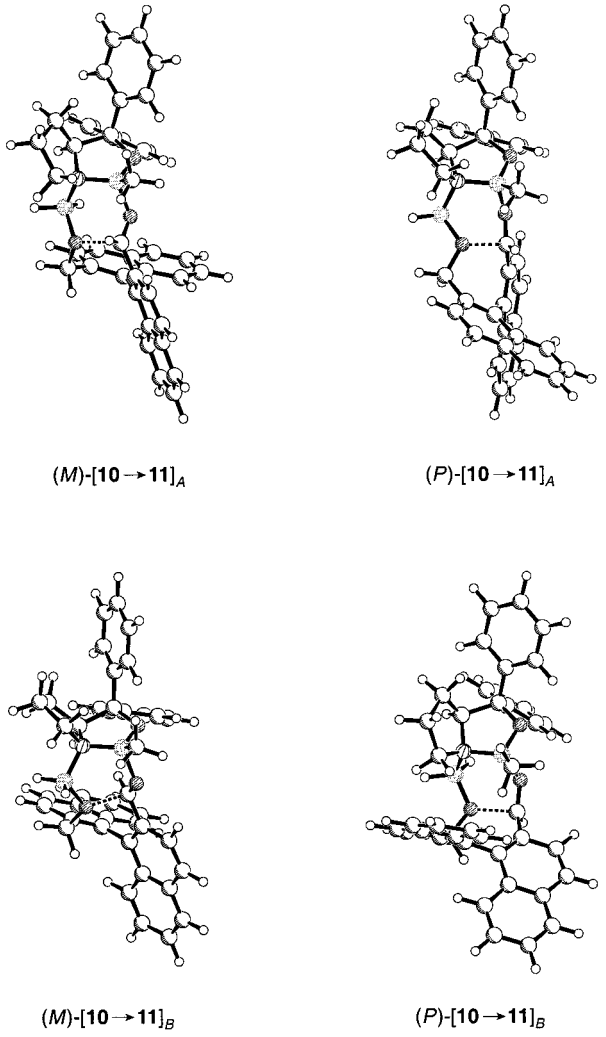


**Figure 5.** Transition structures [**10** → **11**] of the ring opening reaction (step **IV**); disintegrating bond indicated by a dotted line.

8.2 kcal/mol, see Table 2), which is due to the inflexible chiral skeleton of the oxazaborolidine (*S*)-**4** and the large energetic influence of small changes of structural parameters. On the other hand, the difference between the energetically lowest diastereomeric structures of (*M*)-**11** and (*P*)-**11** is only small (0.2 kcal/mol, Table 2), which would allow only a very small atropisomeric differentation if these species could interconvert. The activation barriers for the helimerization processes [(*M*)-**11** ⇌ (*P*)-**11**]$_A$ and [(*M*)-**11** ⇌ (*P*)-**11**]$_B$, however, are high. They were calculated to be 32.7 and 33.4 kcal/mol, respectively, which means that the hydroxy aldehyde derivative **11** is configurationally stable at the biaryl axis, and the stereoselectivity previously attained in step **II** is fully conserved throughout this reaction step.

**Table 5. Second Intramolecular Nucleophilic Attack: Heats of Formation ($\Delta H_f$, kcal/mol), Relative Heats of Formation ($\Delta\Delta H_f$, kcal/mol), Zero Point Energies (ZPE, kcal/mol), Imaginary Frequencies ($\nu_i$, $i$·cm$^{-1}$), Activation Barriers ($\Delta H^{\ddagger}$), and Selected Bond Lengths (Å) of the Energetically Favored Transition Structures [11 → 12]**

| | [11 → 12] | | | |
|---|---|---|---|---|
| | (*M*,*Si*) | (*M*,*Re*) | (*P*,*Si*) | (*P*,*Re*) |
| $\Delta H_f$ | −3.4 | −8.2 | −13.1 | −1.3 |
| $\Delta\Delta H_f$ | 4.8 | ≡ 0 | ≡ 0 | 11.8 |
| $\Delta H^{\ddagger}$ | 6.9 | 10.5 | 5.3 | 12.1 |
| ZPE | 439.4 | 438.8 | 439.1 | 439.0 |
| $\nu_i$ | −492.3 | −417.9 | −585.1 | −440.5 |
| $B_N-O_O$[a] | 1.714 | 1.777 | 1.668 | 1.651 |
| $B_L-H_Q$ | 1.254 | 1.245 | 1.270 | 1.248 |
| $C_J-H_Q$ | 1.697 | 1.734 | 1.599 | 1.770 |

[a] For the atom denotation, see Scheme 4.

**Fifth Fundamental Step: Second Intramolecular Nucleophilic Attack.** The hydroxy aldehyde **11** possesses a new carbonyl function, which is fixed to the *endo* ring boron and is therefore already activated for the second intramolecular nucleophilic hydride transfer (step **V**). In contrast to step **II**, the hydride nucleophile is now provided by a less reactive (since alkoxylated) borane (as part of compound **11**), and the negative charge of the coordinated alkoxyborane is comparable to that of free borane. The lower reactivity is partially overcome by the increased electrophilic nature of the now present aldehyde function of **11**, compared to the ester function in the adduct **8**, and again by the spatially favorable possible position of the hydride for an intramolecular attack. Both effects should accelerate the second hydride transfer step.

This step **V** is strongly exothermic (up to ca. 50 kcal/mol) and shows a distinct *Re*/*Si* differentiation, which, however, does not lead to an additional stereoselectivity since no new stereocenter is generated. In a similar way, the large preference now for a (*P*)-selective attack on **11** (compare Table 5) does not lead to an additional stereodifferentiation, because not only are all previous reaction intermediates **8**−**11** configurationally stable at the biaryl axis, but also the product, dialcohol **12**, again has an activation barrier much higher than required for any helimerization at room temperature ($\Delta H^{\ddagger}$ > 34 kcal/mol), so this does *not* affect the high (*M*)-selectivity obtained by the first irreversible nucleophilic attack (step **II**).

Scheme 7 describes the energetic course of the calculated mechanistic pathway of the stereoselective ring opening reaction of the seven-membered lactone **3** with the chiral oxazaborolidine−$BH_3$ adduct (*S*)-**4**·$BH_3$ from an energetic viewpoint [for every step, only the energetically lowest minimum structures for (*M*)- and (*P*)-isomers and the corresponding transition structures are shown]. This energy diagram visualizes that the two strongly *exo*thermic hydride transfers (steps **II** and **V**) provide the unidirectional driving force for this reaction and compensate the endothermic formation of the adduct com-

**Scheme 7**

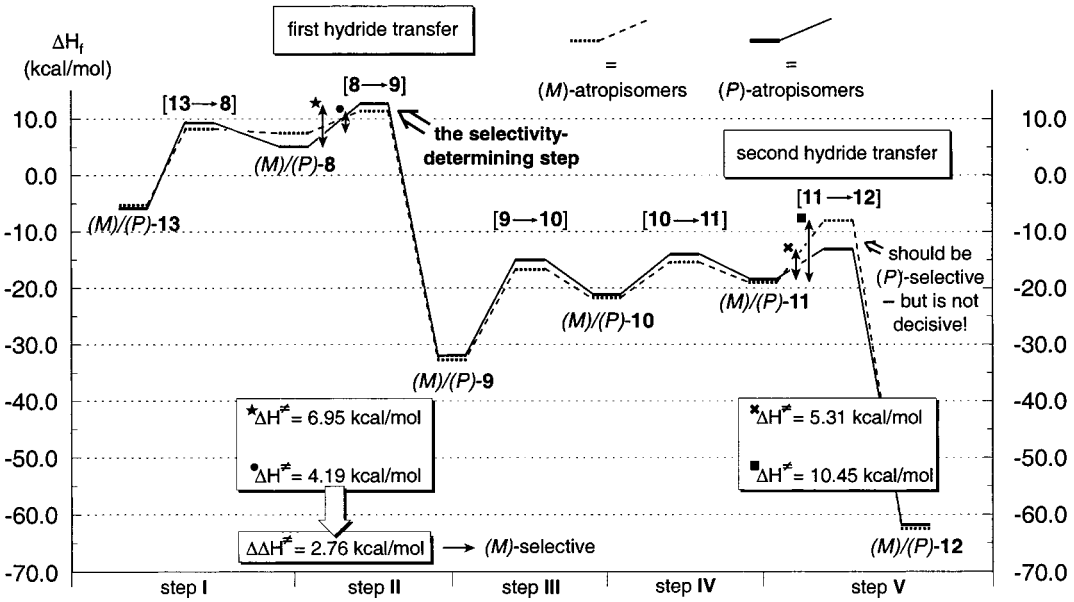


plexes **8** and the likewise endothermic conversion of the lactolate **9** into the hydroxy aldehyde **11** (steps **III** and **IV**). It furthermore shows that the first reduction step is the stereochemically deciding one in the nondynamic kinetic resolution of the racemic lactone **3**.

In summary, this AM1 study corroborates the results obtained experimentally[13] for the oxazaborolidine-mediated borane reduction of the seven-membered biaryl lactone **3** with (*S*)-**4**. Alcohol (*M*)-**5** is formed in a very high enantiomeric excess at the beginning of the kinetic resolution, causing the enrichment of (*P*)-**3** until optical purity. By calculating the complex five-step mechanism, it could be shown that the *first* nucleophilic attack (step **II**) is highly (*M*)-selective (Scheme 3). As this step **II** is irreversible and all reaction intermediates **8**−**12** are configurationally stable concerning the biaryl axis, this selectivity is conserved into the final product (*M*)-**5**. Recently, we could provide experimental evidence that, for the dynamic kinetic resolution of configurationally unstable lactones **6b** and **6c** using BINAL-H as the *H*-nucleophile, the first reduction step is selectivity-determining, too.[7]

Not only the direction of selectivity of this process (*M*) but also the range of stereoselectivity could be calculated with remarkable precision. The energetic differentation in the activation barriers of 2.76 kcal/mol[26] (first nucleophilic attack, step **II**, see Table 3) corresponds to a relative rate constant[27] $k_{rel} = 199$ at −20 °C, which means that the product alcohol (*M*)-**5** should be formed with 99% ee in the beginning of the reaction [experimental result: $k_{rel} = 50$ at −20 °C, 96% initial ee for (*M*)-**5**[13]].[29]

**Extension to the Six-Membered Lactone 6f.** Given the good enantiomeric differentiation ($k_{rel}$ up to 50) for the atroposelective reduction of the seven-membered biaryl lactone **3**, it seemed rewarding to extend the principle to other configurationally stable lactone-bridged biaryls. As a consequence of the shorter bridge, the related six-membered biaryl lactones, when equipped with comparable *ortho*-substituents next to the axis, have distinctly lower atropisomerization barriers,[30] which makes them such attractive substrates for highly enantioselective (e.g., 97% ee for **6c**)[6] reductive ring cleavage reactions by *dynamic* kinetic resolution.[4] Lactone **6f**, however, because of its large *tert*-butyl substituent next to the biaryl axis, has a severely distorted, helicene-like structure and is configurationally stable at room temperature. Despite the great steric hindrance, it has previously been prepared in quite satisfying 31% yield by intramolecular biaryl coupling of the bromo ester **12** using $(Ph_3P)_2PdCl_2$ as the standard catalyst.[30] Encouraged by previous experience in the field of related biaryl lactones,[9,10] we have now improved the coupling yield

(26) The main goal of this study is an improved understanding of the mechanistic course of the reaction and to find out which step is decisive for the experimentally observed selectivity. For the calculation of the relative rate constant and the enantiomeric excess, the theoretical values were used with an accuracy of ±0.01 kcal/mol. It must be noted, however, that the error bars of AM1 calculations are larger than that. Furthermore, the neglect of entropy effects leads to an additional uncertainty of more than 0.01 kcal/mol.

(27) The evaluation of the calculated activation barriers of all possible transition structures (see eq 1) was done according to the Eyring transition state theory,[28] in which some approximations (e.g., the corresponding entropy parts of reactions with similar activation enthalpies are supposed to be equal; consequently, these entropy terms can be neglected) had to be made.

$$\frac{(P)}{(M)} = \frac{k_{(P,Si)} + k_{(P,Re)}}{k_{(M,Si)} + k_{(M,Re)}} = \frac{e^{\frac{-\Delta H^{\ddagger}_{P,Si}}{RT}} + e^{\frac{-\Delta H^{\ddagger}_{P,Re}}{RT}}}{e^{\frac{-\Delta H^{\ddagger}_{M,Si}}{RT}} + e^{\frac{-\Delta H^{\ddagger}_{M,Re}}{RT}}} \qquad (1)$$

(28) (a) Eyring, H. *J. Chem. Phys.* **1935**, *3*, 107. (b) Evans, M. G.; Polanyi, M. *Trans. Faraday Soc.* **1935**, *31*, 875. (c) Wigner, E. *Trans. Faraday Soc.* **1938**, *34*, 29.

(29) Strictly speaking, the *overall* activation barrier from the weakly bonded Coulomb pairs **13** up to the transition structures [**8** → **9**] should be considered for the calculation of the selectivity of the first hydride transfer. Because of its *inter*molecular nature, the formation of the adducts **8** is, however, strongly dependent on solvent effects, in contrast to the following *intra*molecular steps **II** to **V**. As all calculations were performed for the gas phase, the calculation of the first step of this mechanism would give much less reliable data. Therefore, only the relative activation barriers ($\Delta\Delta H^{\ddagger} = 2.76$ kcal/mol corresponding to $k_{rel} = 199$ at −20 °C) of the first hydride transfer (step **II**) itself were considered for the calculation of the relative rate constant. On the basis of the overall reaction (steps **I** plus **II**), the calculated value for $k_{rel}$ would decrease to 2.13 (corresponding to a ratio (*M*)-**9**:(*P*)-**9** = 68:32), hence still predicting the qualitatively right (*M*)-selectivity.

(30) Bringmann, G.; Hartung, T.; Göbel, L.; Schupp, O.; Ewers, C. L. J.; Schöner, B.; Zagst, R.; Peters, K.; von Schnering, H. G.; Burschka, C. *Liebigs Ann. Chem.* **1992**, 225.

**Scheme 8**

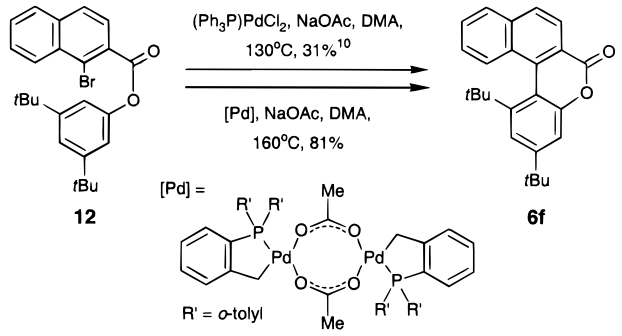


significantly by the use of the Herrmann−Beller catalyst,[31] giving **6f** in an excellent 81% yield (Scheme 8), making this compound a highly hindered and strained but easily attainable substrate for nondynamic kinetic resolution investigations, this time to be *preceded* by quantumchemical mechanistic calculations.

On the basis of the experience from the ring opening of **3**, some simplifying assumptions were made for the calculations on the six-membered lactone **6f**. If, as for **3** and for **6f** itself,[12,32] all reaction intermediates in the reduction of **6f** are configurationally stable at the biaryl axis under the reaction conditions and within the time scale of the reaction course as for all of the other ring cleavage reactions, the first step is the rate-determining one, it should be sufficient to calculate the enantiomer-differentiating capacity of that first hydride transfer step to make a prediction on the sign and the size of the asymmetric induction to be expected. This should reduce the time demand of the calculations enormously. The calculations thus first concentrated on a conformational search of the adduct complexes **15** of **6f** and (*S*)-**4**·$BH_3$ (as resulting from step **I**) and on the course of the first hydride transfer (step **II**) to give lactolates **16** [Scheme 9, arbitrarily formulated for the (*M*)-atropisomeric forms].

The energetically lowest transition structures of the (*M*)- and (*P*)-helimers of the hydride transfer [**15** → **16**] are presented in Scheme 9, and for corresponding parameters see Table 6. The by far lowest activation barrier (3.1 kcal/mol) is found for a *Si* attack on the (*M*)-enantiomer of **6f** from an axial direction, whereas the transition state for the most favorable attack on the (*P*)-helimer of **6f**, which is again preferentially axial (since now coming from the *Re* face), is distinctly (by 2.4 kcal/mol) higher.

The relative energetic difference $\Delta\Delta H^{\ddagger}$ of 2.41 kcal/mol[26] (corresponding to a relative rate constant[27] of $k_{rel}$ = 90 at −20 °C and to a predicted initial er of 98.9:1.1) in favor of the reduction of lactone (*M*)-**6f** implies again a high stereoselectivity already during the first reductive step (see Table 6).[33] The calculation of the helimerization barriers of the three (if any) stereochemically critical species of the five-step mechanism, **16** and the (not shown) analogues of lactol **10** and aldehyde **11**, derived

**Scheme 9**

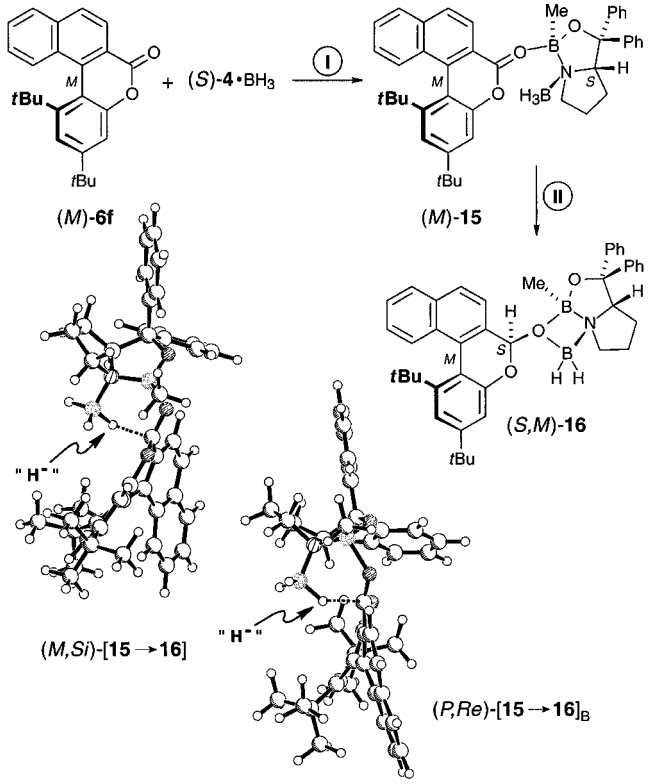


**Table 6. First Intramolecular Nucleophilic Attack: Heats of Formation ($\Delta H_f$, kcal/mol), Relative Heats of Formation ($\Delta\Delta H_f$, kcal/mol), Zero Point Energies (ZPE, kcal/mol), Imaginary Frequencies ($\nu_i$, $i$·cm$^{-1}$), and Activation Barriers ($\Delta H^{\ddagger}$) of the Energetically Favored Transition Structures [15 → 16]**

| | [15 → 16] | | | | |
|---|---|---|---|---|---|
| | (*M*,*Si*) | (*M*,*Re*) | (*P*,*Si*) | (*P*,*Re*)$_A$[b] | (*P*,*Re*)$_B$[b] |
| direction of $H^-$-attack | axial | equatorial | equatorial | axial | axial |
| $\Delta H_f$ | −25.3 | −20.6 | −22.4 | −23.1 | −23.5 |
| $\Delta H^{\ddagger}$ | 3.1 | 7.8 | 6.5 | 5.9 | 5.5 |
| $\Delta\Delta H^{\ddagger}$ | ≡ 0 | 4.7 | 3.4 | 2.8 | 2.4 |
| ZPE | 531.6 | 531.3 | 531.5 | 531.6 | 531.7 |
| $\nu_i$ | −432.9 | −459.6 | −489.6 | −433.2 | −373.5 |
| $B_N-O_O$[a] | 1.726 | 1.715 | 1.691 | 1.756 | 1.751 |
| $B_L-H_P$ | 1.256 | 1.263 | 1.268 | 1.254 | 1.249 |
| $C_J-H_P$ | 1.670 | 1.593 | 1.616 | 1.638 | 1.668 |

[a] For the atom denotation, see Scheme 4. [b] The (*P*,*Re*)-attack was found to pass two transition structures [**15** → **16**], denoted by A and B.

from **6f** as the starting material, revealed relative activation barriers in the same range as calculated for **6f** itself (∼ 25 kcal/mol), indicating these compounds to be configurationally stable at the biaryl axis. Consequently, all other reaction intermediates could likewise be considered as configurationally stable, especially at the reaction temperature of −78 °C. So the calculated ratio for the first hydride transfer of initially 99:1 should be conserved into the final product **7f**.

Encouraged by this computational prediction, the six-membered lactone **6f** was submitted to the same reaction

(31) (a) Herrmann, W. A.; Brossmer, C.; Öfele, K.; Reisinger, C.-P.; Priermeier, T.; Beller, M.; Fischer, H. *Angew. Chem., Int. Ed. Engl.* **1995**, *34*, 1844. (b) Beller, M.; Fischer, H.; Herrmann, W. A.; Öfele, K.; Brossmer, C. *Angew. Chem., Int. Ed. Engl.* **1995**, *34*, 1848.

(32) (*P*)-**6f** had previously been obtained by ring opening of racemic **6f** with chiral *O*-nucleophiles, atropo-diastereomeric resolution, followed by saponification of the stereo-pure esters and subsequent recyclization, though in moderate yields and not fully enantiomerically pure. See: Bringmann, G.; Heubes, M.; Breuning, M.; Göbel, L.; Ochse, M.; Schöner, B., Schupp, O. *J. Org. Chem.*, **2000**, *65*, 722.

(33) If the weakly bonded Coulomb pairs of **6f** and (*S*)-**4**·$BH_3$ are taken as the basis for the calculation of the stereoselectivity of the nondynamic kinetic resolution of **6f** (which was not done here for the reasons given earlier[29]), the calculated enantiomeric ratio at −20 °C decreases from 98.9:1.1 ($k_{rel}$ = 90) to 96.3:3.7 ($k_{rel}$ = 26), still with a preferential reduction of (*M*)-**6f**.

**Scheme 10**

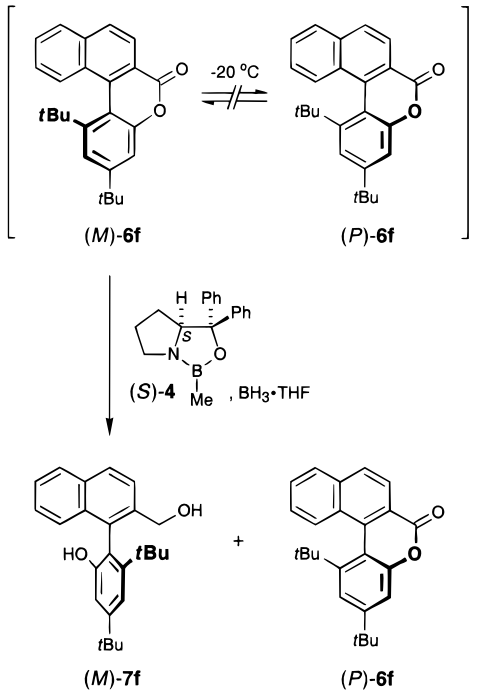


**Table 7. Enantiomeric Ratios[a] (and Corresponding $k_{rel}$ Values) of Reduction of Six- and Seven-Membered Lactones with Borane Activated by Oxazaborolidine (*S*)-4**

| | AM1 calculations | | experimental | |
|---|---|---|---|---|
| | ratio *M*:*P* | $k_{rel}$ [temp] | ratio *M*:*P* | $k_{rel}$ [temp] |
| **6c** | 99.8:0.2 | 499 [25 °C][16] | 98.5:1.5 | 66 [30 °C][6] |
| **3** | 99.5:0.5 | 199 [−20 °C] | 98.0:2.0 | 50 [−20 °C][13] |
| **6f** | 98.9:1.1 | 90 [−20 °C | 97.0:3.0 | 32 [−20 °C] |
| | 99.7:0.3 | 358 [−78 °C] | >99.5:0.5 | >200 [−78 °C] |

[a] The values for configurationally stable lactones **3** and **6f** correspond to the initial enantiomeric ratio, as found at the beginning of the reaction.

conditions with oxazaborolidine (*S*)-**4** and $BH_3$ in THF on an analytical scale at −20 °C (Scheme 10). The samples were worked up immediately and stored at −20 °C until HPLC analysis to avoid any atropisomerization of unreacted **6f**. The relative rate $k_{rel}$ for the kinetic resolution of **6f** by stereoselective oxazaborolidine-assisted borane reduction at −20 °C was determined to be 32 in favor of *M*, with an initial er for (*M*)-**7f**:(*P*)-**7f** of 97:3, i.e., a ratio very close to the predicted one.

At this point, it seemed rewarding to likewise compare the theoretical results for **3** (vide supra) and for the configurationally labile lactone **6c** previously elaborated[16] with the corresponding experimental values[6,13] (see Table 7). In all cases, the AM1 calculations predict correctly predominant (*M*)-selectivity of the cleavage and give a good prediction of the enantioselectivities, which are, as it seems systematically, only slightly higher than the experimental values.

As a result of the high ring strain, **6f** proved to be much more reactive than **3**, thus allowing the ring opening to be conducted even at −78 °C. For this temperature, the calculation would predict a $k_{rel}$ value of even ca. 360, i.e., an er of 99.7:0.3 in favor of the (*M*)-configured cleavage product **7f** (see Table 7). At this low temperature already, oxazaborolidine (*S*)-**4** and $BH_3$, a reagent combination developed for the reduction of aldehydes and ketones,[19]

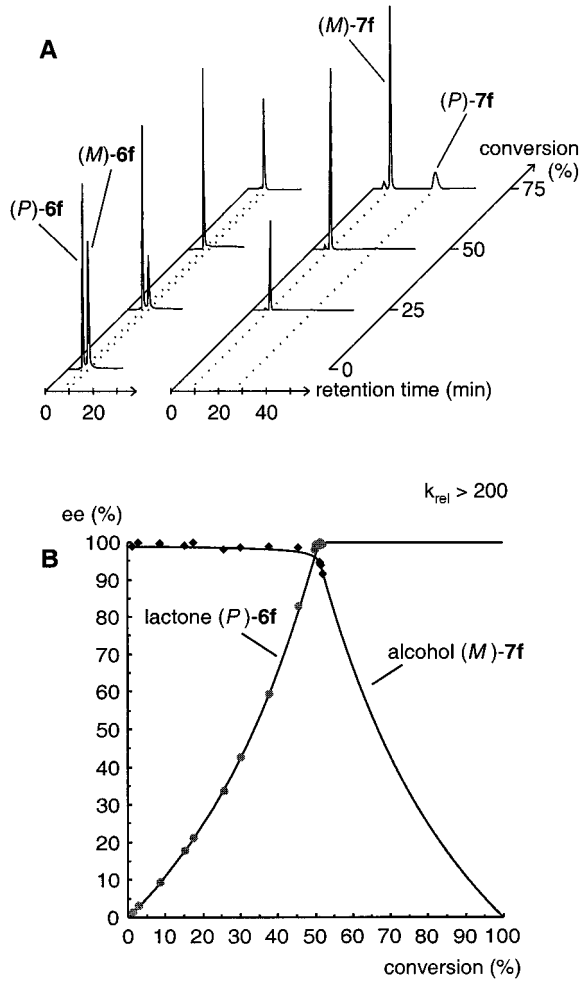


**Figure 6.** The course of the kinetic resolution of lactone **6f**, as shown by (A) HPLC chromatograms at various degrees of conversion and (B) plot of enantiomeric excesses of remaining substrate (*P*)-**6f** and product alcohol (*M*)-**7f** as a function of the conversion.

smoothly reduced the lactone carbonyl function (50% conversion ca. after 1 h, addition of reagent during 1 h). Figure 6 shows the time course of the reaction and the high degree of stereoselectivity obtained in this experiment: the product alcohol (*M*)-**7f** is produced with an initial ee > 99% and with a measured[34] relative rate $k_{rel}$ of more than 200! This permits both the lactone (*P*)-**6f**[6] and the alcohol (*M*)-**7f** to be obtained in very high optical purities (see Figure 6).

Actually, the selectivity obtained for **6f** at −20 °C ($k_{rel}$ = 32) is not as high as for **3** at −20 °C ($k_{rel}$ = 50), it is only the higher reactivity of **6f** that allows the reaction to be conducted at lower temperatures, which in this case leads to the extraordinarily high selectivity observed, in good agreement with the quantum chemical calculations based on a temperature of −78 °C (compare Table 7).

The first samples of the reaction mixture of the ring opening of **6f** at −78 °C contained a considerable amount (up to 10−15%) of the intermediate hydroxy aldehyde **14**.[35] Normally, an aldehyde (here **14**) should react faster

(34) (a) Chen, C.-S.; Fujimoto, Y.; Girdaukas, G.; Sih, C. J. *J. Am. Chem. Soc.* **1982**, *104*, 7294. (b) Kagan, H. B.; Fiaud, J. C. *Top. Stereochem.* **1988**, *18*, 249.

(35) Bringmann, G.; Breuning, M.; Endress, H.; Vitt, D.; Peters, K.; Peters, E.-M. *Tetrahedron* **1998**, *54*, 10677.

**Scheme 11**

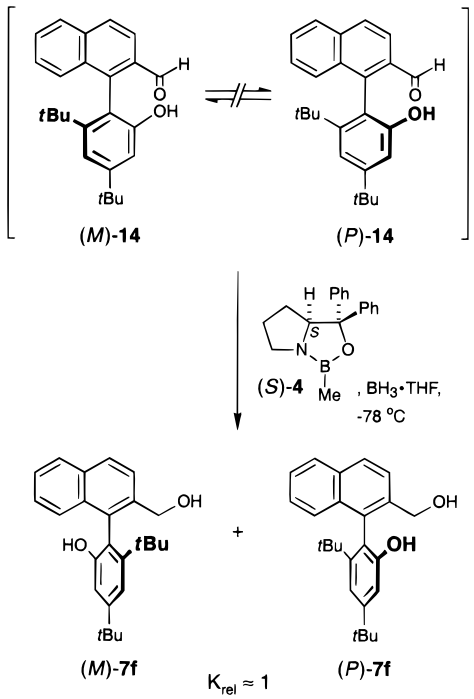


than the corresponding lactone (here **6f**). Here the lactone **6f**, however, is activated by the severe steric strain in the six-membered lactone ring, caused by the bulky *ortho*-substituent, so that the intermediate formation of **14** can be observed in this case.

As to be expected from the mechanistic considerations, this hydroxy aldehyde **14** was found to be (*M*)-configured and showed the same enantiomeric excess as the corresponding (newly formed) alcohol (*M*)-**7f** at the given conversion, which confirms once again that the first step of the ring opening is the selectivity-determining step. This fact was further proven by the attempted kinetic resolution of racemic **14** under the established reaction conditions at −78 °C, leading to nearly racemic **7f** even at the beginning of the reaction ($k_{rel} \approx 1$, see Scheme 11),[36] so that the high stereoselectivity actually attained on the lactone **6f** must result from the first hydride attack.

On a preparative scale (e.g., 290 $\mu$mol of **6f**), the selectivity for the oxazaborolidine-assisted borane reduction of lactone **6f** was still excellent ($k_{rel} \approx 82$), but partial racemization of the lactone (*P*)-**6f** was observed [99% ee before, 95% ee after chromatographic separation from alcohol (*M*)-**7f**], although the complete workup was done at +5 °C (see Experimental Section). Therefore, lactone (*P*)-**6f** was immediately reduced to (*P*)-**7f** (93% ee) after separation from (*M*)-**7f**.

## Conclusions

Semiempirical AM1 studies on the mechanism of the kinetic resolution of configurationally stable biaryl lactones **3** and **6f** by oxazaborolidine-assisted borane reduction revealed that the first, highly (*M*)-selective hydride transfer is the selctivity-determining step of this reaction. The calculated enantioselectivities are in good accordance with the experimental results, which again proves the suitability of the AM1 method for mechanistic studies even on such complex processes. The presented methodology, together with the advantages of the intramolecular Pd-catalyzed biaryl coupling (up to 81% yield even for the highly hindered lactone **6f**), constitutes an excellent and otherwise unattained pathway to prepare enantiomerically pure biaryls with bulky *ortho*-substituents such as *tert*-butyl,[37] in high chemical (for the ring closure and for its cleavage) and optical (for the ring cleavage) yields and (given the availability of **4** in both enantiomeric forms) leading to any desired configuration. High $k_{rel}$ values as found for the kinetic resolution of **6f** are on the edge of chemical processes[38] and approach values normally only found for enzymic reactions.

## Computational Methods

The semiempirical AM1 calculations were performed on Silicon Graphics Indigo (R 4000) and i686-LinuX workstations using the VAMP[39] program (versions 6.1 and 5.5, respectively). The input geometries for the AM1 calculations were obtained using the TRIPOS force field within the SYBYL 6.3 program package.[40] Ground structures were minimized by applying the EF algorithm[41] with a gradient norm specification of 0.1 mdyn/Å, whereas transition structures were optimized by the NS01A algorithm[42] using the corresponding keywords of the VAMP program package. Force calculations were applied to characterize minima and transition structures by calculation of their normal vibrations. In all cases, the correspondence of transition structures to their local minima was determined by IRC calculations.

## Experimental Section

**General.** Melting points are uncorrected. $^1$H NMR spectra were recorded at 250 MHz. For HPLC instrumentation, see Supporting Information. Solvents were dried and purified according to standard procedures. Dimethyl acetamide (DMA) was distilled from $CaH_2$ under argon prior to use. All reactions were carried out under an atmosphere of dry argon.

**Improved Preparation of 1,3-Di-*tert*-butyl-6*H*-benzo[*b*]naphtho[1,2-*d*]pyran-6-one (6f).** A 100 mg (228 $\mu$mol) portion of 3,5-di-*tert*-butylphenyl 1-bromo-2-naphthoate (**12**)[30,43] and 0.21 mg (2.56 $\mu$mol) of NaOAc were dissolved in 10 mL of DMA. The catalyst solution was prepared by dissolving 1.07 mg (1.14 $\mu$mol) of *trans*-di($\mu$-acetato)-bis[*o*-(di-*o*-tolylphosphino)benzyl]dipalladium(II)[31] in 2 mL of DMA. Both solutions were combined in a Schlenk tube and transferred to an oil bath, which had been preheated to 160 °C. Via cannula, the catalyst solution was transferred to the reaction mixture, which was then stirred at 160 °C. The course of the reaction was monitored by TLC (silica, petroleum ether/diethyl ether 10:1). After 3 h, the solvent was removed in vacuo, and the residue was filtered over Celite (petroleum ether/diethyl ether

(36) Under different reaction conditions, the kinetic resolution of racemic **14** with 1.1 equiv of (*S*)-**4** and with catechol borane as the reductant (2.0 equiv in toluene or 0.2 equiv in THF) gave weak preferences in favor of (*P*)-**7f** (er 60:40 and 77:23, respectively) at < 20% conversion (20 °C), see: Bringmann, G.; Breuning, M. *Synlett* **1998**, 634.

(37) For the *non*stereoselective preparation of related 1-(2′-*tert*-butylphenyl)naphthalenes, see i.a. Lesslie, M. S.; Mayer, U. J. H. *J. Chem. Soc.* **1962**, 1401.

(38) For a kinetic resolution of terminal epoxides, with $k_{rel}$ values > 200, see: Larrow, J. F.; Schaus, S. E.; Jacobsen, E. N. *J. Am. Chem. Soc.* **1996**, *118*, 7420.

(39) Rauhut, G.; Chandrasekhar, J.; Alex, A.; Beck, B.; Sauer, W.; Clark, T. *VAMP 6.1*, available from Oxford Molecular Ltd., The Magdalen Centre, Oxford Science Park, Sandford-on-Thames, Oxford OX4 4GA, England.

(40) *SYBYL*; Tripos Associates, 1699 St. Hanley Road, Suite 303, St. Louis, MO, 63144.

(41) (a) Baker, J. *J. Comput. Chem.* **1986**, *7*, 385. (b) Baker, J. *J. Comput. Chem.* **1987**, *8*, 563.

(42) Powell, M. J. D. *Nonlinear Optimization*; Academic Press: New York, 1982.

(43) It is necessary to use **12** in analytically pure form.

10:1). After removal of the solvent, the crude product was purified by column chromatography (silica, petroleum ether/diethyl ether 10:1) and crystallized from petroleum ether/diethyl ether to yield 66.0 mg (184 $\mu$mol, 81%) of **6f** (mp 106−107 °C; lit.[30] 105−107 °C), which was spectroscopically identical to material previously obtained.[30]

**Kinetic Resolution of 1,3-Di-*tert*-butyl-6*H*-benzo[*b*]-naphtho[1,2-*d*]pyran-6-one (6f) and 1-(4′,6′-Di-*tert*-butyl-2′-hydroxyphenyl)naphthalene-2-carbaldehyde (14) (Analytical Scale).** The solution of 26.8 mg (96.6 $\mu$mol) of oxazaborolidine (*S*)-**4** in 1.5 mL of THF was treated with 129 $\mu$L (129 $\mu$mol) of $BH_3$·THF (1.0 M solution in THF) at 0 °C. After 30 min of stirring at room temperature, this solution was added in portions during 1 h to a solution of 32.1 $\mu$mol of lactone **6f**[30] (or hydroxy aldehyde **14**[35]) in 1.5 mL of THF at −78 °C. For HPLC analysis, 100 $\mu$L of the reaction mixture was quenched with 2 N HCl and immediately extracted with diethyl ether. The organic solution was purified by TLC to yield samples of **6f** and **7f** (or **14** and **7f**), which were stored at −20 °C until HPLC examination.

**Kinetic Resolution of 6f (Preparative Scale).** Similarly, the preformed solution of 241 mg (869 $\mu$mol) of (*S*)-**4** and 4 equiv of $BH_3$·THF in 6 mL of THF was cooled and added dropwise during 2 h to 104 mg (290 $\mu$mol) of racemic **6f** in 6 mL of THF at −78 °C. The course of the reaction was monitored by HPLC. After 3 h, the reaction mixture was quenched by cautious addition of 5 mL of $H_2O$ and 5 mL of 2 N HCl and extracted with 5 × 15 mL of chilled $CH_2Cl_2$. At this point, i.e., before isolation, the unreacted lactone (*P*)-**6f** was found to be enantiomerically pure (99% ee) according to HPLC analysis. During the following workup, the temperature did not exceed +5 °C. After drying of the organic phase over anhydrous $Na_2SO_4$, rapid removal of the solvent in vacuo and column chromatography (silica, petroleum ether/diethyl ether 2:1) provided 41.9 mg (117 $\mu$mol, 40%) of (*P*)-**6f** (95% ee) and 61.1 mg (169 $\mu$mol, 58%) of (*M*)-**7f** (68% ee). Under similar conditions, the kinetic resolution of **6f** gave 48.7 mg (136 $\mu$mol, 47%) of (*P*)-**6f** (97% ee) and 51.1 mg (141 $\mu$mol, 49%) of (*M*)-**7f** (90% ee) after a reaction time of 80 min (52% conversion).

**(*P*)-1,3-Di-*tert*-butyl-6*H*-benzo[*b*]naphtho[1,2-*d*]pyran-6-one [(*P*)-6f]:** colorless oil, 97% ee; $[\alpha]^{23}_D = -109.6$ (*c* 0.41, $CHCl_3$) (lit.[32] −63.1, *c* 0.50, $CHCl_3$).

**(*M*)-1-(2-Hydroxy-4,6-di-*tert*-butylphenyl)-2-naphthalenemethanol [(*M*)-7f]:** colorless oil, 90% ee; spectroscopically identical to material previously obtained in racemic form;[44] $[\alpha]^{23}_D = -20.1$ (*c* 0.51, $CHCl_3$).

**(*P*)-1-(2-Hydroxy-4,6-di-*tert*-butylphenyl)-2-naphthalenemethanol [(*P*)-7f].** To 41.9 mg (117 $\mu$mol) of (*P*)-**6f** (95% ee) in 8 mL of THF was added 8.88 mg (234 $\mu$mol) of $LiAlH_4$ at 0 °C. After 16 h of stirring at 0 °C, the reaction mixture was carefully quenched by addition of 1 mL of $H_2O$ and acidified with 2 N HCl. After extraction with $CH_2Cl_2$, the organic phase was dried over $Na_2SO_4$, the solvent was removed in vacuo, and the residue was purified by column chromatography (silica, petroleum ether/diethyl ether 1:1) to provide 35.3 mg (97.4 $\mu$mol, 83%) of (*P*)-**7f** (93% ee): colorless oil; $[\alpha]^{23}_D = 21.6$ (*c* 0.88, $CHCl_3$).

**Acknowledgment.** This work has been supported by the Deutsche Forschungsgemeinschaft (SFB 347 “Selektive Reaktionen Metall-aktivierter Moleküle”) and by the Fonds der Chemischen Industrie. J.H. thanks the Freistaat Bayern for a generous fellowship. Valuable suggestions by Prof. B. Engels, University of Würzburg, are gratefully acknowledged.

**Supporting Information Available:** Details of the chromatographic resolution of **6f**, **7f**, and **14**; minimum structures of weakly bonded Coulomb pairs **13**; table of selected dihedral angles of compounds **8**−**13**; and *Z*-matrices and total energies of all compounds calculated (60 pages). This material is available free of charge via the Internet at http://pubs.acs.org.

JO991729X

(44) (a) Bringmann, G.; Hartung, T.; Göbel, L.; Schupp, O.; Peters, K.; von Schnering, H. G. *Liebigs Ann. Chem.* **1992**, 769. (b) Peters, K.; Peters, E.-M.; von Schnering, H. G.; Bringmann, G.; Hartung, T. *Z. Kristallogr.* **1994**, *209*, 740.